DØ Note 5894-CONF

Search for Tau Sneutrino particles in the $e + \mu$ final state at DØ

The DØ Collaboration
URL http://www-d0.fnal.gov
(Dated: March 13, 2009)

This note describes a search for R-parity violating (RPV) sneutrinos in the $e\mu$ final state in 3.1 fb^{-1} of DØ Run IIb data, collected at the Fermilab Tevatron $p\bar{p}$ collider from June 2006 to December 2008. Good agreement between the data and the Standard Model background prediction is observed. Since there is no evidence for new physics, we combine this result with the Run IIa 1 fb^{-1} results to set 95% C.L. limits on the production cross section times branching ratio ($\sigma \times BR(\tilde{\nu}_\tau \rightarrow e\mu)$) and RPV couplings $\lambda'_{311} \times \lambda_{312}$ for different sneutrino masses.

I. INTRODUCTION

In supersymmetry (SUSY), the R parity which differentiates standard model particles from their supersymmetric partners could be violated in the most general representation of the superpotential which includes R parity violationg (RPV). [1].

$$\mathcal{W}_{\not R_p} = \frac{1}{2}\varepsilon_{ab}\lambda_{ijk}L_i^a L_j^b E_k + \varepsilon_{ab}\lambda^{'}_{ijk}L_i^a Q_j^b D_k + \frac{1}{2}\varepsilon_{\alpha\beta\gamma}\lambda^{''}_{ijk}U_i^\alpha D_j^\beta D_k^\gamma + \varepsilon_{ab}\delta_i L_i^a H_2^b \tag{1}$$

Through the first two terms LLE and LQD in the superpotential, a single scalar neutrino $\tilde{\nu}$ can be produced, and subsequently decay into the lepton flavor violating (LFV) $e\mu$ channel. The Feynman diagram is shown in Fig. 1.

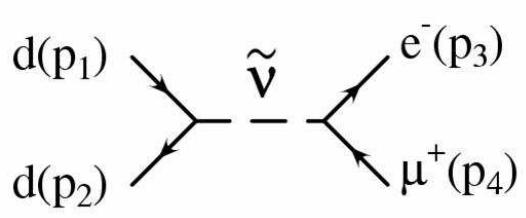

FIG. 1: The Feynman diagram of tau sneutrino $e\mu$ resonance production in hadron collisions

The search is performed under the single dominance hypothesis [2] that the third-generation sneutrino $\tilde{\nu}_\tau$ is the lightest supersymmetric particle (LSP) and dominantly produced by assuming that all RPV couplings but $\lambda^{'}_{311}$ and $\lambda_{312} = \lambda_{321}$ are zero. Consequently, the cross section of the signal only depends on the third generation sneutrino mass M and the LQD and LLE coupling constants, as [3]

$$\hat{\sigma}_{e\mu} \propto (\lambda^{'}_{311})^2 \times (\lambda_{312})^2 \cdot \frac{1}{|\hat{s} - M^2 + i\Gamma M|^2}, \tag{2}$$

where the total width of the LSP sneutrino Γ, determined by decay modes $d\bar{d}$ and $e\mu$ solely, can be written as

$$\Gamma = [3 \cdot (\lambda^{'}_{311})^2 + 2 \cdot \lambda^2_{312}] \cdot \frac{M}{16\pi} \tag{3}$$

The indirect two standard deviation bounds on the coupling constants and the mass of tau sneutrino are given by Ref.[4]

$$\lambda^{'}_{311} \leq 0.12, \quad \lambda_{312} \leq 0.07, \quad for\ M \equiv M_{\tilde{\nu}_\tau} \geq 100\ GeV \tag{4}$$

This set of parameters will be used as default for demonstration purpose unless explicitly stated otherwise.

In this note, a direct search on sneutrino particle via $e + \mu$ final states based on 3.1 fb^{-1} Run IIb data is presented. We combine it with our Run IIa publication results [5] to set more stringent limits on RPV couplings.

II. DØ DETECTOR AND DATA SAMPLE

The DØ detector is described in detail elsewhere [6]. The central-tracking system consists of a silicon microstrip tracker (SMT) and a central fiber tracker (CFT) which has eight thin coaxial barrels, each supporting two doublet layers. Both of the SMT and CFT are located within a 2 Tesla superconducting solenoidal magnet, with designs optimized for tracking and vertexing at pseudorapidities $|\eta| < 3$ and $|\eta| < 2.5$, respectively. Outside the solenoid, a 3-layer scintillating strip detector (CPS) provides a precise measurement of electromagnetic (EM) shower positions. The surrounding liquid argon and uranium calorimeter consists of a central section (CC) which covers pseudorapidities $|\eta|$ up to 1.1, and two end calorimeters (EC) that extend coverage to $|\eta| \sim 4.2$, with all three housed in separate cryostats. Each section consists of an inner electromagnetic (EM) compartment, followed by a hadronic compartment. The muon system covers a pseudorapidity of $|\eta| < 2$ and consists of a layer of tracking detectors and scintillation trigger counters in front of 1.8 Tesla toroids, followed by two similar layers after the toroids. Luminosity is measured using plastic scintillator arrays located in front of the EC cryostats, covering $2.7 < |\eta| < 4.4$. The data acquisition system consists of a three-level trigger, designed to accommodate the high instantaneous luminosity.

The data sample used in this analysis was collected between June 2006 and December 2008 using single or dilepton events. For final states containing one electron with transverse energy E_T above 30 GeV and one muon with transverse momentum p_T above 25 GeV, the trigger efficiency is close to 100%.

III. EVENT SELECTION

The electron selection requires (i) an EM cluster with a cone of radius $\Delta R = \sqrt{(\Delta\phi)^2 + (\Delta\eta)^2} = 0.2$ in the central calorimeter ($|\eta_{det}| < 1.1$), with transverse energy $E_T > 30$ GeV, where E_T is defined as the cluster energy times sinθ, and θ is the polar angle with respect to the proton beam direction; (ii) at least 90% of the cluster energy be deposited in the EM section of the calorimeter; (iii) the calorimeter isolation variable (I) be less than 0.15, where $I = \frac{E_{tot}(0.4)-E_{EM}(0.2)}{E_{EM}(0.2)}$, $E_{tot}(0.4)$ is the total energy in a cone of radius 0.4, and $E_{EM}(0.2)$ the EM energy in a cone of radius 0.2 around the electron candidate direction; (iv) an artificial neural network variable (ANN) based on information sensitive to differences between EM objects and jets in the tracker activity and in the energy distributions in the calorimeter and CPS be consistent with that of electrons; and (v) a track pointing to the EM cluster. The reconstruction efficiency of electrons, as determined from a $Z \to e^+e^-$ data sample, is about 75%.

The muon candidate is required to be separated from the electron candidate by $\Delta R > 0.2$ and from any jets by $\Delta R > 0.5$, where jets are reconstructed using an iterative seed-based cone algorithm [7]. In addition, we require (i) that the track p_T be above 25 GeV; (ii) hits in the muon scintillation counters with time be consistent with originating from the proton-antiproton collision; (iii) at least 8 CFT hits along the track; (iv) the E_T sum of the calorimeter cells in the annular cone of $0.1 < \Delta R < 0.4$ be less than 2.5 GeV, and the transverse momentum sum of all tracks besides the muon track within a cone of radius $\Delta R = 0.5$ be less than 2.5 GeV. The reconstruction efficiency of muons determined from a $Z \to \mu^+\mu^-$ data sample is about 77%.

The tracks of the two leptons are required to originate from the same vertex. To suppress the WW and $t\bar{t}$ backgrounds, events with missing transverse energy $\not\!\!E_T > 20$ GeV that is not aligned or antialigned in azimuth with the muon ($0.7 < \Delta\phi(\not\!\!E_T, \mu) < 2.5$ rad), as well as events with at least one jet with $p_T > 25$ GeV and $|\eta| < 2.5$ are rejected.

IV. BACKGROUND AND SIGNAL SIMULATION

The main background contributions are from $Z \to \tau\tau$, WW/WZ, W+jet inclusive and $t\bar{t}$ processes that decay to $e\mu$ final states. The SM Monte Carlo (MC) samples used in this analysis are generated using PYTHIA [8] except for the W+jet samples (which are generated with ALPGEN [9], and showered using PYTHIA) with CTEQ6L [10] parton distribution functions (PDFs) , and processed through a GEANT-3 based [11] simulation of the DØ detector and the same reconstruction software as the data. All the background contributions are normalized using the NLO or NNLO theoretical cross sections and are re-weighted to correct for different distributions of instantaneous luminosity and primary vertex position in z in data and MC samples. In addition, the $Z \to \tau\tau$ and W+jet samples are re-weighted to match the Z and W p_T spectrum in data.

The COMPHEP [12] generator is used to generate the hard scattering processes of the signal, which are interfaced to PYTHIA for showering and then passed through a detailed detector simulation and the same reconstruction code as used for data.

V. RESULTS

The event selection criteria are applied to data and MC samples. Table I shows the relative systematic uncertainties of this analysis. The number of selected events in data and the estimated background contributions are summarized in Table II. The final kinematic distributions are shown in Fig. 2.

Sources	Uncertainties(%)
luminosity	6.1 [13]
trigger	0.1
electron identification efficiency	2.3
muon identification efficiency	2.3
$Z/\gamma* \rightarrow ll$ cross section	3.5 [14]
WW incl. cross section	6.6 [15]
WZ incl. cross section	2.7 [15]
$t\bar{t}$ incl. cross section	14.8 [16]
W+jet/γ cross section	8.5 [17]
PDF for signal acceptance	0.4-0.6

TABLE I: Systematic uncertainties, expressed as fractions of the expected event yield.

Process	No. of events
$Z/\gamma*$	83.4 ± 6.8
diboson	46.0 ± 4.0
$t\bar{t}$ incl.	2.6 ± 0.5
W+jet/γ	12.7 ± 2.5
total backgroud	144.9 ± 8.3
data	143

TABLE II: The number of selected events in the data and different estimated background contributions. Uncertainties on backgrounds cover both systematic and statistical.

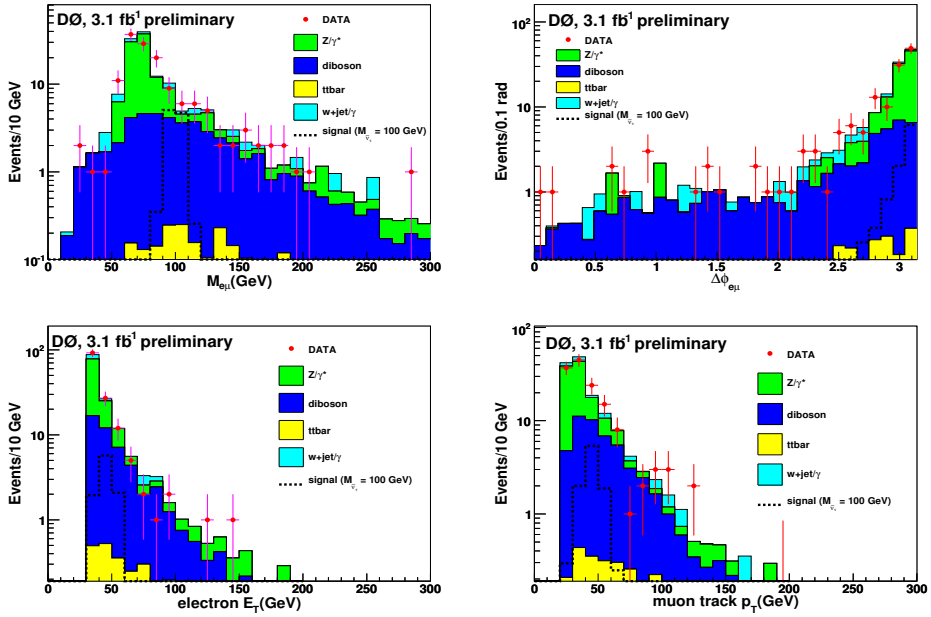

FIG. 2: Distributions of the electron muon invariant mass and azimuth difference (top row) and of the electron transverse energy and muon transverse momentum (bottom row) for data (points with error bars), background simulation (histograms) and expected signal for $M_{\tilde{\nu}_\tau} = 100$ GeV and $\sigma \times BR = 21$ fb.

Since there is no evidence for new physics, we proceed to set upper limits on the sneutrino production cross section times branching ratio for sneutrino decaying into one electron and one muon and RPV couplings $\lambda'_{311} \times \lambda_{312}$ for different sneutrino masses. The distribution of electron and muon invariant mass (shown in Fig. 2) is used for this purpose. Limits are calculated at the 95% confidence level using the modified frequentist CLs approach with a Poisson log-likelihood ratio test statistic [18]. The impact of systematic uncertainties is incorporated via convolution of the Poisson probability distributions corresponding to the different sources of systematic uncertainty. The correlation in systematic uncertainties are maintained between signal and backgrounds. We combine the Run IIa 1.0 fb^{-1} results with the current Run IIb results. The corresponding graphs are displayed in Fig. 3.

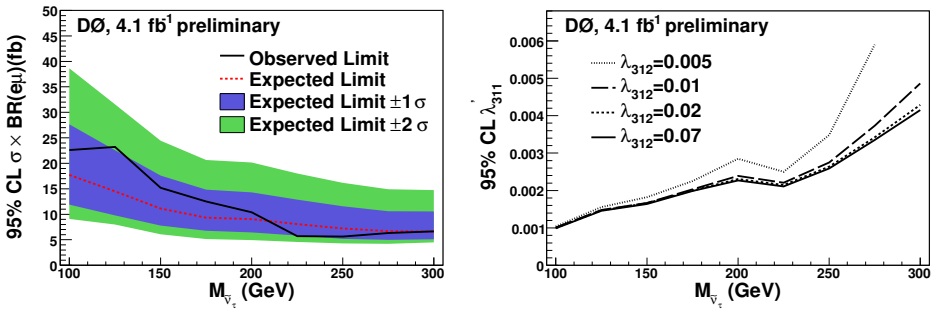

FIG. 3: 95% C.L. limits on $\sigma\times$ BR (left) and RPV couplings (right) as a function of the sneutrino mass with using 4.1 fb^{-1} of DØ Run II data.

VI. SUMMARY

This note describes a search for the production of high p_T electron muon pairs in proton antiproton collisions using 3.1 fb^{-1} of DØ Run IIb data, collected at the Fermilab Tevatron collider from June 2006 to December 2008. Good agreement between the data and the Standard Model background prediction is observed, as 143 events are selected in the data while the SM expectation is 144.9 ± 8.3 events. Since there is no evidence for new physics, we combine it with the Run IIa 1 fb^{-1} results to set 95% C.L. limits on the production cross section times branching ratio and RPV couplings $\lambda'_{311} \times \lambda_{312}$ for different sneutrino masses.

Acknowledgments

We thank the staffs at Fermilab and collaborating institutions, and acknowledge support from the DOE and NSF (USA); CEA and CNRS/IN2P3 (France); FASI, Rosatom and RFBR (Russia); CAPES, CNPq, FAPERJ, FAPESP and FUNDUNESP (Brazil); DAE and DST (India); Colciencias (Colombia); CONACyT (Mexico); KRF and KOSEF (Korea); CONICET and UBACyT (Argentina); FOM (The Netherlands); STFC (United Kingdom); MSMT and GACR (Czech Republic); CRC Program, CFI, NSERC and WestGrid Project (Canada); BMBF and DFG (Germany); SFI (Ireland); The Swedish Research Council (Sweden); CAS and CNSF (China); and the Alexander von Humboldt Foundation.

[1] S. Weinberg, Phys. Rev. **D26** (1982) 287; N. Sakai, T. Yanagida, Nucl. Phys. **B197** (1982) 533.
[2] M.Chetob, Prog. Part. Nucl. Phys. **54**, (2005)71.
[3] Y.B. Sun et al., Commun. Theor. Phys. **44**, 107 (2005), arXiv:hep-ph/0412205
[4] R. Barbieri *et al.*, hep-ph/9810232; B. Allanach et al., hep-ph/9906224;
F. Deliot et al, Phys. Lett.**B475** (2000)184;
G. Moreau et al. Nucl. Phys. **B604** (2001)3;
S. Bar-Shalom, G. Eilam and B. Mele,Phys. Rev. **D64** (2001) 095008.
[5] V.M. Abazov *et al.*, (DØ Collaboration), Phys. Rev. Lett. **100**, 241803 (2008).
[6] V.M. Abazov *et al.*, (DØ Collaboration), "The upgraded DØ detector",Nucl. Instrum. Methods Phys. Res. **A565**, 463 (2006).

[7] G.C. Blazey *et al.*, in Proceedings of the Workshop QCD and Weak Boson Physics in Run II, edited by U. Baur, R.K. Ellis and D.Zeppenfeld, Fermilab-Pub- 00/297 (2000), arXiv:hep-ex/0005012
[8] T. Sjöstrand *et al.*, Comput. Phys. Commun. **135**, 238 (2001).
[9] M. Mangano *et al.*, ALPGEN arXiv:hep-ph/0206293, JHEP07 (2003) 001, version 2.05, http://mlm.web.cern.cn/mlm/alpgen
[10] J. Pumplin *et al.*, JHEP **0207**, 012 (2002).
[11] R. Brun and F. Carminati, CERN Program Library Long Writeup W5013,1993 (unpublished).
[12] A. Pukhov *et al.*, INP MSU Report No. 98-41/542.
[13] T. Andeen et al., FERMILAB-TM-2365 (2007).
[14] R. Hamberg, W. L. van Neerven, and T. Matsuura, Nucl. Phys. **B359**, 343 (1991) [Erratum-ibid. **644**, 403 (2002)].
[15] J. M. Campbell and R. K. Ellis, Phys. Rev. **D60**, 11306 (1999).
[16] M. Cacciari,S. Frixione, M. L. Mangano,P. Nason and G. Ridolfi. J High Energy Phys. **0404**, 068(2004).
[17] V.M. Abazov *et al.*, (DØ Collaboration), arXiv:hep-ex/0810.3873.
[18] W. Fisher, FERMILAB-TM-2386-E (2006).